



Thermally induced evolution of hydrogenated amorphous carbon

Filippo Mangolini, Franck Rose, James Hilbert, and Robert W. Carpick

Citation: [Applied Physics Letters](#) **103**, 161605 (2013); doi: 10.1063/1.4826100

View online: <http://dx.doi.org/10.1063/1.4826100>

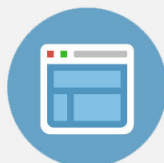
View Table of Contents: <http://scitation.aip.org/content/aip/journal/apl/103/16?ver=pdfcov>

Published by the [AIP Publishing](#)



Re-register for Table of Content Alerts

Create a profile.



Sign up today!



Thermally induced evolution of hydrogenated amorphous carbon

Filippo Mangolini,¹ Franck Rose,² James Hilbert,³ and Robert W. Carpick^{3,a)}

¹Department of Materials Science and Engineering, University of Pennsylvania, Philadelphia, Pennsylvania 19104, USA

²HGST, a Western Digital Company, San Jose, California 95135, USA

³Department of Mechanical Engineering and Applied Mechanics, University of Pennsylvania, Philadelphia, Pennsylvania 19104, USA

(Received 3 August 2013; accepted 2 October 2013; published online 17 October 2013)

The thermally induced structural evolution of hydrogenated amorphous carbon (a-C:H) films was investigated *in situ* by X-ray photoelectron spectroscopy for annealing temperatures up to 500 °C. A model for the conversion of sp³- to sp²-hybridized carbon in a-C:H vs. temperature and time was developed and applied to determine the ranges of activation energies for the thermally activated processes occurring. The energies are consistent with ordering and clustering of sp² carbon, scission of sp³ carbon-hydrogen bonds and formation of sp² carbon, and direct transformation of sp³- to sp²-hybridized carbon. © 2013 AIP Publishing LLC. [<http://dx.doi.org/10.1063/1.4826100>]

The thermally induced structural evolution of amorphous carbon (a-C) thin films is a subject of fundamental and technological interest.^{1–4} As one example, knowledge of the temperature effects on the structure of a-C coatings, which are used as overcoat material in hard-disk drives to protect the magnetic medium against corrosion and wear,⁵ is fundamental for the development of one of the most promising solutions for increasing the magnetic storage density, namely, heat-assisted magnetic recording (HAMR).⁶ The intensive localized heating employed in HAMR for data encoding raises concerns about the structural changes occurring in a-C overcoats. The investigation of thermally induced evolution of the structure of a-C thin films is difficult experimentally due to the challenging nature of quantifying the bonding configuration of carbon in these materials.^{7,8} Thermally induced changes are important for hydrogen-free tetrahedral amorphous carbon (ta-C), since post-deposition annealing (usually for a few minutes at ~650 °C) is required to relieve the high compressive stress (2–8 GPa) typical for these films.⁹ The thermally induced stress relaxation was modeled by Sullivan *et al.* as a series of first order chemical reactions leading to the conversion of fourfold-coordinated (sp³) carbon atoms into threefold-coordinated (sp²) carbon atoms.⁹ Because of bond length and angle disorder in ta-C, Sullivan *et al.* postulated the presence of a distribution of activation energies for sp³-to-sp² conversion of carbon hybridization, which was found to range between 1 eV and 3 eV. The model of Sullivan *et al.* was applied by Grierson *et al.* to determine an activation energy range for the thermally induced sp³-to-sp² conversion of carbon hybridization in ta-C by analyzing near edge X-ray absorption fine structure spectra.² The activation energy calculated by Grierson *et al.* (3.5 ± 0.9 eV)² was in agreement with the activation energy for bulk sp³-to-sp² conversion of carbon hybridization in ta-C derived from Raman spectroscopic measurements (3.3 eV).¹⁰ The small fraction of sp²-hybridized carbon in ta-C was postulated to act like defects in the sp³-hybridized carbon matrix, which can

diffuse and form larger clusters upon annealing.¹⁰ The activation energy for the clustering of sp² carbon in the sp³ carbon matrix (0.28 eV) was calculated to be much lower than that for sp³-to-sp² conversion.¹⁰

The presence of hydrogen in amorphous carbon reduces the thermal stability.⁸ Although the basic processes governing the temperature-induced modifications in hydrogenated amorphous carbon (a-C:H), namely, the evolution of hydrogen followed by formation of sp²-hybridized carbon, have already been identified,^{8,11} no previous studies presented a quantitative evaluation of the energetics of this process. Such studies are challenging for thin films since several techniques that can measure carbon hybridization, such as Raman or nuclear magnetic resonance spectroscopy, are bulk techniques. Thus, surface-sensitive analytical methods that can provide information on carbon hybridization are desirable.

Thin a-C:H films (HGST, San Jose, CA, USA) were deposited on 63.5-mm-diameter glass disks coated with a 20 nm-thick NiTa adhesion layer using plasma-enhanced chemical vapor deposition.⁴ The film density and thickness, determined by X-ray reflectivity, were 2.1 ± 0.1 g/cm³ (Ref. 4) and 30.0 ± 0.2 nm, respectively. The hydrogen content, measured by hydrogen forward scattering (Evans Analytical Group, Sunnyvale, CA, USA), was 26 ± 3 at.%. The chemistry and structure of the near-surface region was investigated by X-ray photoelectron spectroscopy (XPS) using a customized XPS spectrometer (VG Scienta AB, Uppsala, Sweden).¹² XPS analyses were performed using a monochromatic Al K α source (photon energy: 1486.6 eV). The residual pressure in the analysis chamber was always $< 1 \times 10^{-6}$ Pa. The spectrometer was calibrated according to ISO 15472:2001 with an accuracy of ± 0.05 eV. Binding-energies are the means over three independent measurements with corresponding standard deviations. Survey and high-resolution spectra were acquired in constant-analyzer-energy mode with pass energies of 200 eV and 100 eV, respectively. The full width at half-maximum (FWHM) of the peak-height for the high-resolution Ag_{3d5/2} signal of a sputter-cleaned Ag sample was 0.57 eV. The spectra were processed using CasaXPS software (v2.3.16, Casa Software Ltd., Wilmslow, Cheshire, UK).

^{a)}Author to whom correspondence should be addressed. Electronic mail: carpick@seas.upenn.edu

Background subtraction was performed using the Shirley-Sherwood method.¹³ The quantitative evaluation of XPS data, as described in Refs. 14 and 15, was based on integrated intensity using a first-principles model and applying Powell's equations.¹⁶ The inelastic-mean-free-path was calculated using the Tanuma, Powell, and Penn (TPP-2M) formula.¹⁷

To investigate the structural evolution of a-C:H vs. temperature, heating experiments were performed inside the XPS chamber. The samples ($6 \times 6 \text{ mm}^2$) were mounted in a holder (RHK Technology, Inc., Troy, MI, USA) that included a tungsten filament for radiative heating and a K-type thermocouple in contact with the sample for recording specimen temperature. The films were annealed in progressive steps from 150 °C to 500 °C at 50 °C intervals for 1 h and cooled after each anneal (heating and cooling rate: 10 °C/min). The XPS spectra were acquired after cooling the sample to below 40 °C after each heating step.

The survey spectrum of unannealed a-C:H (not shown) exhibited the characteristic signals of carbon (C_{1s} at approximately 285 eV and C_{KVV} Auger feature at 1224 eV).¹⁸ Weak oxygen signals (O_{1s} at 533 eV and O_{KVV} Auger feature at 974 eV) were also detected.¹⁸ The high-resolution C_{1s} signal (information depth for photoelectrons with kinetic energy of 1202.6 eV: 9.5 nm) of unannealed a-C:H (Figures 1(a) and 1(b)) was fit using the C_{1s} reference spectra of freshly cleaved highly ordered pyrolytic graphite (HOPG, grade 2, SPI Supplies, West Chester, PA, USA) and hydrogen-terminated ultrananocrystalline diamond (UNCD (95% sp^3 -bonded carbon¹⁹), Advanced Diamond Technologies, Romeoville, IL, USA). This confirmed that the binding energy values of the C_{1s} transition for sp^2 -bonded carbon and highly sp^3 -bonded carbon are identical ($284.5 \pm 0.1 \text{ eV}$).^{7,20} Using assignments from reliable literature, we identify five components of the C_{1s} signal of unannealed a-C:H (Figures 1(a) and 1(b)): $284.51 \pm 0.05 \text{ eV}$ (a-C:H); $285.00 \pm 0.05 \text{ eV}$ (aliphatic contamination^{18,21}—due to air exposure); and $286.52 \pm 0.08 \text{ eV}$, $287.87 \pm 0.09 \text{ eV}$, and $289.27 \pm 0.05 \text{ eV}$ (carbon bound to oxygen^{21,22}—contamination due to air exposure). The C_{1s} spectrum also exhibited an energy loss structure between 290

and 330 eV, due to plasmon oscillations of ($\sigma + \pi$) valence electrons.²⁰ The curve synthesis of the plasmon band (Figure 1(c)) was carried out employing the peak-fitting parameters derived from reference materials (HOPG and UNCD). The peaks from sp^2 - and sp^3 -hybridized carbon and contributing to the plasmon band of a-C:H were summed into two envelopes in Figure 1(c). The high-resolution O_{1s} spectrum of unannealed a-C:H was fit with three components: 531.60 ± 0.05 and 532.64 ± 0.05 (oxygen bonded to carbon²¹); and $534.00 \pm 0.05 \text{ eV}$ (adsorbed water¹⁸) (Figure 1(d)). The X-ray induced C_{KVV} Auger spectrum (information depth for photoelectrons with kinetic energy of 261.6 eV: 3.3 nm) of a-C:H is displayed in Figure 1(e) together with its first derivative. The C_{KVV} spectrum yields information about the electronic structure of carbon allotropes.^{23,24} In particular, the distance D between the most positive maximum and most negative minimum in the first derivative C_{KVV} spectrum is linearly proportional to the fraction of sp^2 -hybridized carbon (f_{sp^2}).^{7,20,24–31} In the present work, a linear fit of the published D values measured for a series of carbon allotropes^{7,20,25–31} allowed the sp^2 fraction in a-C:H to be determined ($f_{sp^2} = 0.53 \pm 0.04$). The Auger measurement samples more surface contamination than the XPS due to the shallower information depth; it also has a poorer signal-to-noise ratio. Regardless, these Auger results agree, within uncertainty, with the sp^2 carbon fraction calculated from the intensity ratio of the components assigned to sp^2 and sp^3 carbon in the plasmon band near the C_{1s} peak ($f_{sp^2} = 0.51 \pm 0.01$).

The high-resolution spectra of a-C:H annealed at different temperatures are also displayed in Figure 1. To properly calibrate the C_{1s} peak intensities for annealed samples, the total area of the C_{1s} peaks assigned to carbon bound to oxygen (Figures 1(a) and 1(b)) were set equal to the total area of the peaks for oxygen bound to carbon obtained from fitting the O_{1s} spectrum (Figure 1(d)). Upon annealing, the intensities of the peaks assigned to aliphatic carbon and to carbon bonded to oxygen progressively decreased (Figure 2(a)), suggesting desorption of a contamination layer present on a-C:H, whose presence is expected due to the prior exposure

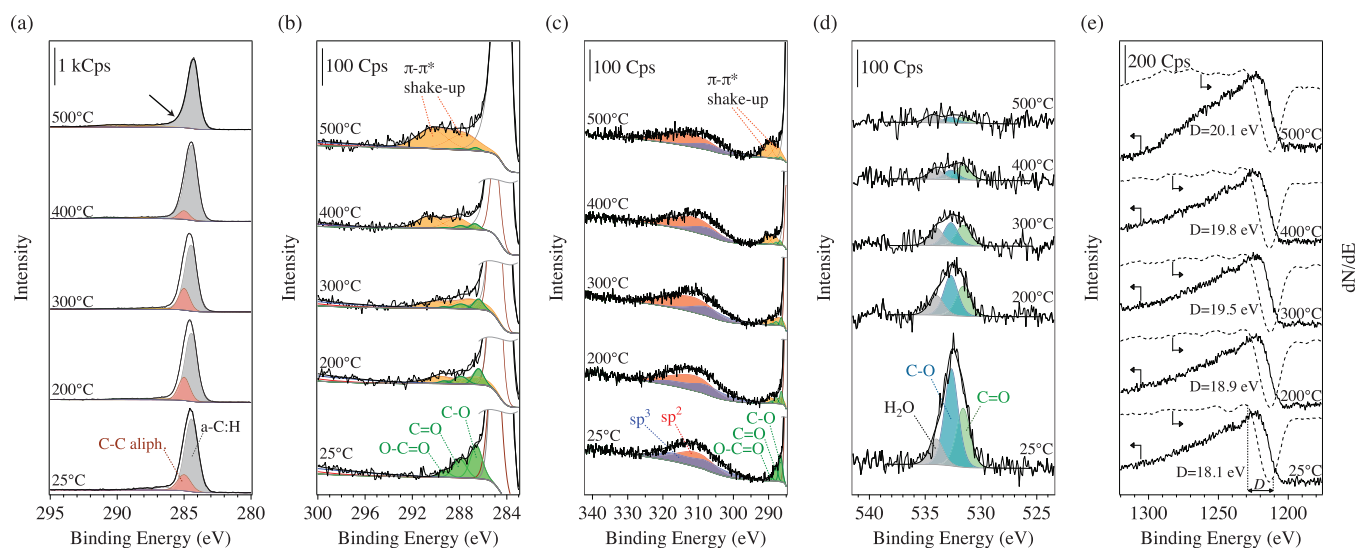


FIG. 1. XPS spectra of a-C:H acquired before annealing, and after annealing at different temperatures. Colored lines are curve fits. (a) and (b) C_{1s} , (c) plasmon band, (d) O_{1s} , (e) C_{KVV} Auger feature (solid lines) with its first derivative (dashed lines).

of the samples to air. The C_{1s} spectra (Figure 1(a)) also exhibited a change in lineshape upon annealing: while at room temperature the a-C:H peak could be described by means of a symmetric Gaussian-Lorentzian function, a good fit to data acquired after annealing could only be achieved by introducing a tail on the high binding-energy side of the synthetic curve (see arrow, Figure 1(a)). The asymmetry of the C_{1s} signal increased with the annealing temperature, while the FWHM decreased. The curve synthesis of the C_{1s} spectra of a-C:H annealed at 200 °C and higher exhibited two new components at 287.7 ± 0.2 eV and at 290.4 ± 0.2 eV (Figure 1(b)). These peaks, assigned to the characteristic π - π^* shake-up satellites in ordered sp^2 -hybridized carbon,^{32,33} increased in intensity with annealing temperature (Figure 2(b)). The appearance of these peaks, together with the increased lineshape asymmetry of the C_{1s} peak, suggests a progressive ordering of the sp^2 carbon sites with a reduction of the dihedral angle between π electrons.^{32,33}

The clustering and ordering of sp^2 carbon sites were postulated to derive from the sp^2 carbon sites acting like

defects in a sp^3 carbon matrix.¹⁰ To provide experimental evidence that this clustering in a-C:H is a thermally activated process, the ratio of the intensity of the π - π^* shake-up satellites to that of the a-C:H synthetic peak is displayed in an Arrhenius plot (inset, Figure 2(b)). A model based on an Arrhenius equation that includes a Gaussian distribution of activation energies, fits the experimental data well (correlation coefficient: 0.87), better than a fit with a single activation energy (correlation coefficient: 0.85). The quality of both fits suggests that the clustering of sp^2 sites is a single, rate-limited thermally activated process. According to the fit with the Gaussian distribution, the activation energy range for sp^2 clustering in a-C:H is 0.18 ± 0.05 eV.

The curve synthesis of the plasmon band (Figure 1(c)) indicates a progressive change of the relative fractions of sp^2 - and sp^3 -hybridized carbon upon annealing. The sp^2 fraction vs. temperature is displayed in Figure 2(c). This fully agrees, within experimental uncertainty, with the fraction of sp^2 -hybridized carbon calculated from the peak-to-peak width in the C_{KVV} first derivative spectra. In the following,

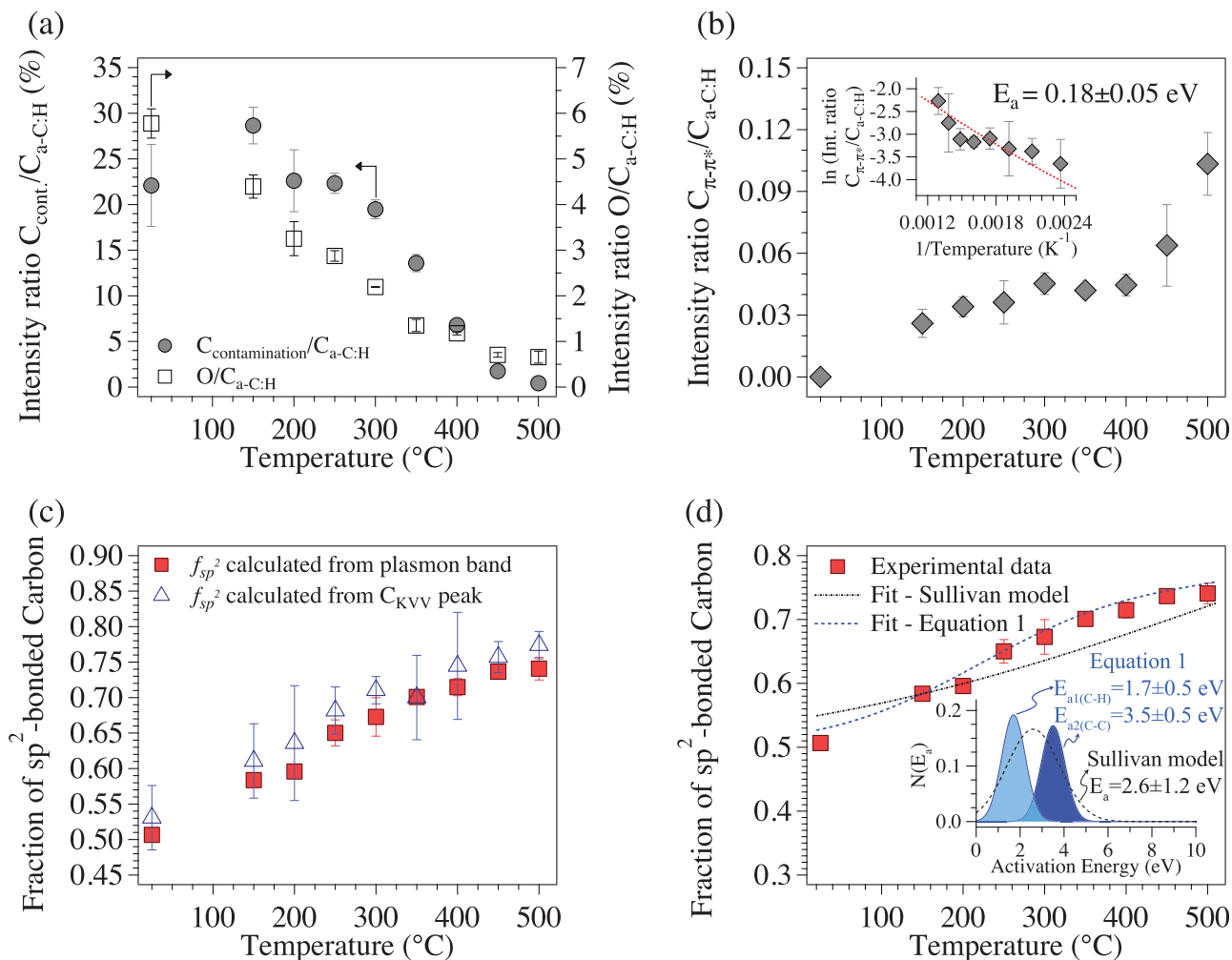


FIG. 2. (a) Intensity of carbon (aliphatic, $\underline{C-O}$, $\underline{C=O}$, $\underline{O-C=O}$) and oxygen ($\underline{C-O}$, $\underline{C=O}$, $\underline{H_2O}$) signals in the contamination layer on a-C:H relative to the $C_{a-C:H}$ signal vs. annealing temperature under high-vacuum conditions; (b) intensity ratio between the π - π^* shake-up satellites and the a-C:H synthetic peak vs. annealing temperature, indicating thermally induced clustering of sp^2 -hybridized carbon sites. Inset: Arrhenius plot of this intensity ratio; (c) fraction of sp^2 -hybridized carbon vs. annealing temperature calculated both by fitting the plasmon band near the C_{1s} peak (filled red squares) and by determining the distance between the most positive maximum and most negative minimum in the first derivative of the C_{KVV} spectrum (open blue triangles); (d) fraction of sp^2 -hybridized carbon (calculated by fitting the plasmon band near the C_{1s} peak) vs. annealing temperature. The experimental data were fit with the model of Sullivan *et al.* (see Ref. 9) (black dotted line) and with Eq. (1) (blue dashed line). Inset: the corresponding distributions of activation energies for sp^3 -to- sp^2 conversion.

the fraction of sp^2 -bonded carbon derived from the fitting of the plasmon band near the C_{1s} signal will be used for modeling the evolution of a-C:H upon annealing.

The model of Sullivan *et al.*⁹ for describing the transformation of sp^3 to sp^2 carbon in ta-C involves an expression for the conversion *vs.* temperature and time under the assumption that rehybridization only requires thermal activation over an energy barrier, i.e., is governed by first order reaction rate theory. Because of bond length and angle disorder in ta-C, Sullivan *et al.* postulated a distribution of activation energies for sp^3 -to- sp^2 conversion. The variation of sp^2 fractions *vs.* annealing temperature was fit assuming the distribution of activation energies for sp^3 -to- sp^2 conversion to be Gaussian, and using the mean and standard deviation of the Gaussian distribution as fitting parameters. The fitting of the present data (Figure 2(d)) yielded an activation energy distribution for sp^3 -to- sp^2 conversion of 2.6 ± 1.2 eV. The correlation coefficient is low (0.81) and the result unrealistically predicts

a significant fraction of sp^3 -hybridized carbon able to convert to sp^2 hybridization at room temperature. This suggests that the Sullivan model for ta-C cannot describe the thermally induced sp^3 -to- sp^2 conversion of carbon in a-C:H.

A model, based on a refinement of the Sullivan model and accounting for the presence of hydrogen in a-C:H, is presented here. Under the assumption, that all the hydrogen atoms in a-C:H are bonded to sp^3 carbon atoms and that the transformation from sp^3 to sp^2 is governed by first order reaction rate theory independent of the element bonded to fourfold carbon atoms, a new expression for the amount of sp^2 -hybridized carbon as a function of time and temperature $sp^2(t, T)$ was derived. Two thermally activated processes for sp^3 -hybridized carbon sites are assumed: conversion to sp^2 hybridization (as with ta-C) and, for those carbon atoms bonded to one hydrogen atom, the scission of the carbon-hydrogen bond to form sp^2 -hybridized carbon. The resulting equation is

$$sp^2(t, T) = sp^2(0, RT) + sp_{C-H}^3(0, RT) \int \int N_1(E_{a1}) \left[1 - \exp\left(-v_0 \tilde{t} \exp\left(-\frac{E_{a1}}{k_B \tilde{T}}\right)\right) \right] dE_{a1} d\tilde{t} d\tilde{T} \\ + sp_{C-C}^3(0, RT) \int \int N_2(E_{a2}) \left[1 - \exp\left(-v_0 \tilde{t} \exp\left(-\frac{E_{a2}}{k_B \tilde{T}}\right)\right) \right] dE_{a2} d\tilde{t} d\tilde{T}, \quad (1)$$

where $sp^2(0, RT)$ is the sp^2 fraction for unannealed a-C:H, $sp_{C-x}^3(0, RT)$ is the fraction of sp^3 carbon bonded to x for unannealed a-C:H ($x = H$ or C), $N_1(E_{a1})$ is the probability distribution of the sp^3 fraction of carbon-hydrogen bonds versus activation energy (E_{a1}), $N_2(E_{a2})$ is the probability distribution of the sp^3 fraction of carbon-carbon bonds versus activation energy (E_{a2}), v_0 is the attempt frequency typical for solid state reactions (chosen to be 10^{13} s^{-1} (Ref. 9)), and k_B is Boltzmann's constant. $N_1(E_{a1})$ and $N_2(E_{a2})$ were assumed to be Gaussian distributions with equal standard deviations and were normalized to set their areas equal to $sp_{C-H}^3(0, RT)$ and $sp_{C-C}^3(0, RT)$, respectively.

The experimental data could be well fit by Eq. (1) (correlation coefficient: 0.98) using the mean of each Gaussian distribution and their standard deviation as fitting parameters (Figure 2(d)). This analysis yielded a mean activation energy E_{a1} for sp_{C-H}^3 -to- sp^2 conversion (i.e., scission of a carbon-hydrogen bonds to form sp^2 -hybridized carbon sites) of 1.7 ± 0.5 eV and a mean activation energy E_{a2} for sp_{C-C}^3 -to- sp^2 conversion (i.e., transformation of sp^3 -hybridized carbon to sp^2 hybridization) of 3.5 ± 0.5 eV. The activation energy range for sp^3 -to- sp^2 conversion of carbon-carbon bonds in a-C:H agrees with the activation energy necessary for directly converting sp^3 -hybridized into sp^2 -hybridized carbon in ta-C (3.5 ± 0.9 eV (Ref. 2) or 3.3 eV (Ref. 10)), indicating that hydrogen has no significant effect on the energetics of rehybridization. However, the significant amount of hydrogen results in the presence of a second distribution of activation energies with a lower mean value that represents C-H bond scission. This provides the

first quantitative energetic analysis for the lower thermal stability of a-C:H compared to H-free materials.

In conclusion, the thermally induced structural evolution of a-C:H can be probed *in situ* by XPS. Upon high vacuum annealing, three thermally activated processes with an assumed Gaussian distribution of activation energies with mean value E and standard deviation σ occur in a-C:H: (a) ordering and clustering of sp^2 -hybridized carbon ($E = 0.18$ eV; $\sigma = 0.05$ eV); (b) scission of sp^3 carbon-hydrogen bonds with subsequent formation of sp^2 -hybridized carbon ($E = 1.7$ eV; $\sigma = 0.5$ eV); and (c) direct transformation of sp^3 - to sp^2 -hybridized carbon ($E = 3.5$ eV; $\sigma = 0.5$ eV). This first XPS-based study quantifying the energetics of the thermally induced structural evolution of a-C:H demonstrates both the low absolute energy barrier for clustering of the sp^2 phases, and indicates that hydrogen enables conversion to sp^2 hybridization in these films. While the techniques used are sensitive to the near-surface region, the information depths (3.3 and 9.5 nm for X-ray induced Auger spectroscopy (XAES) and XPS, respectively) would probe the entirety of technologically relevant film thicknesses for hard-disk applications (< 2 nm). We do not hypothesize that the near-surface region of the film studied here behaves any differently than the rest of the film, particularly since no oxidation occurs in the vacuum environment.

This material is based upon work supported by the Advanced Storage Technology Consortium ASTC (Grant No. 2011-012) and the National Science Foundation under Grant No. DMR-1107642. F.M. acknowledges support from the Marie Curie International Outgoing Fellowship for

Career Development within the 7th European Community Framework Programme under Contract No. PEOF-GA-2012-328776. We acknowledge Dr. Tevis D. B. Jacobs from the University of Pennsylvania, Department of Materials Science and Engineering, for fruitful discussions and valuable suggestions.

- ¹S. Anders, J. Diaz, J. W. Ager, R. Y. Lo, and D. B. Bogy, *Appl. Phys. Lett.* **71**, 3367 (1997).
- ²D. S. Grierson, A. V. Sumant, A. R. Koniczek, T. A. Friedmann, J. P. Sullivan, and R. W. Carpick, *J. Appl. Phys.* **107**, 033523 (2010).
- ³S. Takabayashi, K. Okamoto, H. Sakaue, T. Takahagi, K. Shimada, and T. Nakatani, *J. Appl. Phys.* **104**, 043512 (2008).
- ⁴N. Wang, K. Komvopoulos, F. Rose, and B. Marchon, *J. Appl. Phys.* **113**, 083517 (2013).
- ⁵C. M. Mate, *Tribology on the Small Scale - A Bottom Up Approach to Friction, Lubrication, and Wear* (Oxford University Press, Oxford, 2007).
- ⁶M. H. Kryder, E. C. Gage, T. W. McDaniel, W. A. Challener, R. E. Rottmayer, J. Ganping, H. Yiao-Tee, and M. F. Erden, *Proc. IEEE* **96**, 1810 (2008).
- ⁷S. Kaciulis, *Surf. Interface Anal.* **44**, 1155 (2012).
- ⁸J. Robertson, *Mater. Sci. Eng. R.* **37**, 129 (2002).
- ⁹J. P. Sullivan, T. Friedmann, and A. Baca, *J. Electron. Mater.* **26**, 1021 (1997).
- ¹⁰A. C. Ferrari, S. Rodil, J. Robertson, and W. Milne, *Diamond Relat. Mater.* **11**, 994 (2002).
- ¹¹L. Calliari, M. Filippo, G. Gottardi, N. Laidani, and M. Anderle, *Surf. Interface Anal.* **38**, 761 (2006).
- ¹²F. Mangolini, J. Åhlund, G. E. Wabiszewski, V. P. Adiga, P. Egberts, F. Streller, K. Backlund, P. G. Karlsson, B. Wannberg, and R. W. Carpick, *Rev. Sci. Instrum.* **83**, 093112 (2012).
- ¹³D. A. Shirley, *Phys. Rev. B* **5**, 4709 (1972).
- ¹⁴F. Mangolini, Ph.D. dissertation (Swiss Federal Institute of Technology (ETH), Zurich, 2011).
- ¹⁵F. Mangolini, A. Rossi, and N. D. Spencer, *J. Phys. Chem. C* **115**, 1339 (2011).
- ¹⁶C. J. Powell, in *Quantitative Surface Analysis of Materials*, edited by N. S. McIntyre (American Society for Testing and Materials, Philadelphia, USA, 1978), p. 5.
- ¹⁷S. Tanuma, in *Surface Analysis by Auger and X-Ray Photoelectron Spectroscopy*, edited by D. Briggs and J. T. Grant (IM Publications, Chichester, UK, 2003), p. 259.
- ¹⁸J. F. Moulder, W. F. Stickle, P. W. Sobol, and K. D. Bomben, *Handbook of X-ray Photoelectron Spectroscopy* (Perkin-Elmer Corporation, Physical Electronics Division, Eden Prairie, MN, USA, 1992).
- ¹⁹A. R. Koniczek, D. S. Grierson, P. U. P. A. Gilbert, W. G. Sawyer, A. V. Sumant, and R. W. Carpick, *Phys. Rev. Lett.* **100**, 235502 (2008).
- ²⁰A. Mezzi and S. Kaciulis, *Surf. Interface Anal.* **42**, 1082 (2010).
- ²¹G. Beamson and D. Briggs, *High Resolution XPS of Organic Polymers: The Scienta ESCA300 Database* (John Wiley & Sons, Chichester, UK, 1992).
- ²²M. Yang, M. J. Marino, V. J. Bojan, O. L. Aryilmaz, A. Erdemir, and S. H. Kim, *Appl. Surf. Sci.* **257**, 7633 (2011).
- ²³D. E. Ramaker, in *Surface Analysis by Auger and X-Ray Photoelectron Spectroscopy*, edited by D. Briggs and J. T. Grant (IM Publications, Chichester, UK, 2003), p. 465.
- ²⁴F. R. McFeely, S. P. Kowalczyk, L. Ley, R. G. Cavell, R. A. Pollak, and D. A. Shirley, *Phys. Rev. B* **9**, 5268 (1974).
- ²⁵S. T. Jackson and R. G. Nuzzo, *Appl. Surf. Sci.* **90**, 195 (1995).
- ²⁶J. C. Lascovich, R. Giorgi, and S. Scaglione, *Appl. Surf. Sci.* **47**, 17 (1991).
- ²⁷J. C. Lascovich and S. Scaglione, *Appl. Surf. Sci.* **78**, 17 (1994).
- ²⁸Y. Mizokawa, T. Kiyasato, S. Nakamura, K. M. Geib, and C. W. Wilmsen, *Surf. Sci.* **182**, 431 (1987).
- ²⁹I. Montero, L. Galán, A. Laurent, J. Perrière, and J. Spousta, *Thin Solid Films* **228**, 72 (1993).
- ³⁰S.-C. Seo and D. C. Ingram, *J. Vac. Sci. Technol. A* **15**, 2579 (1997).
- ³¹J. Zemek, J. Zalman, and A. Luches, *Appl. Surf. Sci.* **133**, 27 (1998).
- ³²G. Kovach, A. Karacs, G. Radnoczi, H. Csorbai, L. Guzzi, M. Veres, M. Koox, L. Papadimitriou, A. Sólyom, and G. Pető, *Appl. Surf. Sci.* **254**, 2790 (2008).
- ³³J. A. Leiro, M. Heinonen, T. Laiho, and I. Batirev, *J. Electron Spectrosc. Relat. Phenom.* **128**, 205 (2003).